THE UNIVERSITY of EDINBURGH

Edinburgh Research Explorer

Can a spreading flame over electric wire insulation in concurrent flow achieve steady propagation in microgravity?

Citation for published version:
Nagachi, M, Mitsui, F, Citerne, J-M, Dutilleul, H, Guibaud, A, Jomaas, G, Legros, G, Hashimoto, N & Fujita, O 2018, 'Can a spreading flame over electric wire insulation in concurrent flow achieve steady propagation in microgravity?', *Proceedings of the Combustion Institute*, pp. 4155-4162. https://doi.org/10.1016/j.proci.2018.05.007

Digital Object Identifier (DOI):
10.1016/j.proci.2018.05.007

Link:
Link to publication record in Edinburgh Research Explorer

Document Version:
Peer reviewed version

Published In:
Proceedings of the Combustion Institute

General rights
Copyright for the publications made accessible via the Edinburgh Research Explorer is retained by the author(s) and / or other copyright owners and it is a condition of accessing these publications that users recognise and abide by the legal requirements associated with these rights.

Take down policy
The University of Edinburgh has made every reasonable effort to ensure that Edinburgh Research Explorer content complies with UK legislation. If you believe that the public display of this file breaches copyright please contact openaccess@ed.ac.uk providing details, and we will remove access to the work immediately and investigate your claim.

Download date: 05. May. 2023

Can a spreading flame over electric wire insulation in concurrent flow achieve steady propagation in microgravity?

Masashi Nagachi[a], Fumiya Mitsui[a], Jean-Marie Citerne[b], Hugo Dutilleul[b], Augustin Guibaud[b]

Grunde Jomaas[c,d], Guillaume Legros[b], Nozomu Hashimoto[a], Osamu Fujita[a*]

[a]Hokkaido University, Sapporo, Hokkaido, 066-8628, Japan
[b]Sorbonne Université, Centre National de la Recherche Scientifique, UMR 7190, Institut Jean Le Rond d'Alembert, F-75005 Paris, France
[c]School of Engineering, University of Edinburgh, EH9 3FG, Edinburgh, United Kingdom
[d]Department of Civil Engineering, Technical University of Denmark, 2800 Kgs. Lyngby, Denmark

[*]Corresponding author. Fax: +81 11706 6385. E-mail address: ofujita@eng.hokudai.ac.jp (O. Fujita).

Colloquium: Fire research

Total length of the paper: 6188 (Method 1)

Equations: 76
Main text: 2838
References: 542
Fig. 1: 415
Fig. 2: 166
Fig. 3: 258
Fig. 4: 439
Fig. 5: 437
Fig. 6: 156
Fig. 7: 163
Fig. 8: 160
Fig. 9: 160
Fig. 10: 377

Abstract

Concurrent flame spread over electric wire insulation was studied experimentally in microgravity conditions during parabolic flights. Polyethylene insulated Nickel-Chrome wires and Copper wires were examined for external flow velocities ranging from 50 mm/s to 200 mm/s. The experimental results showed that steady state flame spread over wire insulation in microgravity could be achieved, even for concurrent flow. A theoretical analysis on the balance of heat supply from the flame to the unburned region, radiation heat loss from the surface to the ambient and required energy to sustain the flame propagation was carried out to explain the presence of steady spread over insulated wire under concurrent flow. Based on the theory, the change in heat input (defined by the balance between heat supply from flame and radiation heat loss) was drawn as a function of the flame spread rate. The curve intersected the linear line of the required energy to sustain the flame. This balance point evidences the existence of steady propagation in concurrent flow. Moreover, the estimated steady spread rate (1.2 mm/s) was consistent with the experimental result by considering the ratio of the actual flame length to the theoretical to be 0.5. Further experimental results showed that the concurrent flame spread rate increased with the external flow velocity. In addition, the steady spread rate was found to be faster for Copper wires than for Nickel-Chrome wires. The experimental results for upward spreading (concurrent spreading) in normal gravity were compared with the microgravity results. In normal gravity, the flame did not reach a steady state within the investigated parameter range. This is due to the fact that the fairly large flame spread rate prevented the aforementioned heat balance to be reached, which meant that such a spread rate could

not be attained within the length of the tested sample.

Keywords

Flame spread rate, Concurrent flow, Microgravity, Electrical wire, Fire safety in space

1. Introduction

Fire safety in space is one of the most important requirements for manned space missions [1]. A likely fire cause in spacecrafts is ignition and flame spread over the wire insulation that is used in the numerous electric devices. Therefore, it is important to understand the ignition and fire behavior in microgravity, especially at the low flow velocities associated with spacecraft ventilation. Various aspects of wire insulation combustion in microgravity have been studied, such as ignition limit, flame spread rate, and extinction limit of numerous materials under various conditions [2-14]. Furthermore, in a recent review paper, the most flammable conditions in microgravity were identified [15]. However, there are few research results on concurrent flame spread over wire insulation in microgravity, even though this flow condition is considered most hazardous [16].

Concurrent flow flames (normal gravity equivalent is upward propagation) spread faster and are thus considered more dangerous than opposed flow flame propagation (normal gravity equivalent is downward propagation). The main difference is due to the greater extent of preheating of the unburned material ahead of the pyrolysis front. Thus, from the perspective of fire safety, observing flame spreading phenomena under concurrent flow is one of the most important problems.

In previous research, flame propagation in concurrent flow has been considered to be an acceleration process, because the flame length determines the magnitude of the heat feedback to the preheat zone, and this heat transfer is closely related to the flame spread rate. Thus, if the flame spread rate increases, the flame length increases and it increases the heat feedback, which in turn leads to an increase in the flame spread rate. In other words, the size of the flame (and the heat

release rate from the flame) increases as a function of time [17–19]. However, cases resulting in steady spread in concurrent flow for flat samples have recently been published, e.g. for fabric sheet [20], chromatography sheet [21], Kimwipes [22] and cotton-fiberglass [23]. Also, according to Honda et al. [24], propagation over solid fuel beds under concurrent flow becomes steady because of transverse heat loss or radiation loss from the sample surface. Moreover, according to numerical simulation results by T'ien, steady flame spread in concurrent flow can be achieved using infinitely wide samples [25]. In the case of wires, the extinction limit for concurrent flame spread over wire insulation in microgravity was obtained experimentally and predicted using scaling analysis [16]. However, there is still limited research focusing on concurrent flame propagation phenomena over wire insulation in microgravity.

Herein, concurrent flame spread in microgravity will be presented for insulated wires in various oxygen concentrations and flow velocities. In particular, the study focuses on whether the flame spread over the wire insulation reaches a steady state or not.

2. Experimental Configuration

Figure 1a shows the experimental setup for the parabolic flight experiments and the normal gravity experiments. The cylindrical part of chamber has an inner diameter of 190 mm. In the combustion chamber, the oxidizer flow entered from the bottom and was vented at the top. The oxidizer velocity was controlled by mass flow controllers. A detailed description of the experimental design and method and further information is available from Citerne et al. [5]. The backlight was turned on/off

with fixed intervals. As a result the camera not only captured the direct flame emission, but also the image with a backlight, which was used to visualize the behavior of molten insulation and the soot distribution in the flame. Also, further research to measure the soot volume fraction and temperature using this camera is ongoing [26]. The pressure inside the chamber was always set to 1 atmosphere using a Rapid Control Valve (This valve allows exhaust flow rates up to 1800 NL/min).

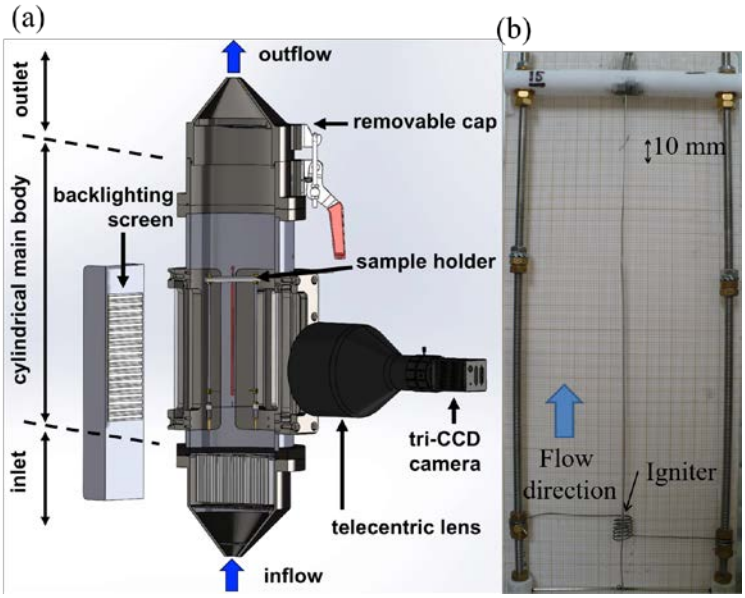

Fig. 1. Experimental setup: (a) schematic cut of the combustion chamber; (b) picture of a sample on a sample holder.

Figure 1b shows a picture of a sample holder. Every sample holder had a wire coated with 116 mm of polyethylene. In this study, two types of core wires were used, namely Nickel-chrome (NiCr) and Cupper (Cu). The core diameter was 0.5 mm and the insulation thickness was 0.3 mm. For the ignition procedure, an 8 mm coil made from 0.5 mm diameter Kanthal wire was set to encircle (6 times) the upstream end of the sample wire, and the coil produced approximately 94 W for 8 seconds. The ignition sequence was initiated before the start of the microgravity period, so that the actual

ignition occurred during microgravity. According to T'ien's flat sheet experiments on the International Space Station [23], steady flame lengths were achieved after about 20s. The microgravity environment was therefore carried out during parabolic flights (on board of the Novespace A310 airplane), which enabled microgravity conditions for about 22 seconds for each parabola.

3. Results

3.1. Flame images

Figure 2 shows a typical flame image where the external flow and flame spread direction is from left to right. The flame tip is defined as the downstream edge of the luminous flame in Fig. 2 and the flame base is defined as the upstream edge of the luminous flame in Fig. 2. The flame length is defined as the length of the luminous flame, i.e. the distance between the flame tip and the flame base.

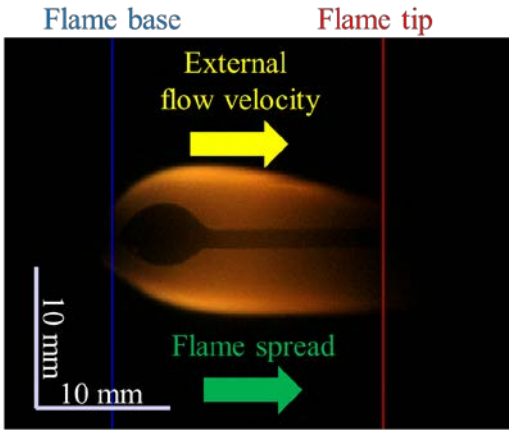

Fig. 2. Typical frame showing the shape of the flame spreading in a concurrent flow (velocity: 150 mm/s; O_2 concentration: 18%).

Figure 3 shows the flame shape of the wire insulation for different flow velocities and oxygen concentrations.

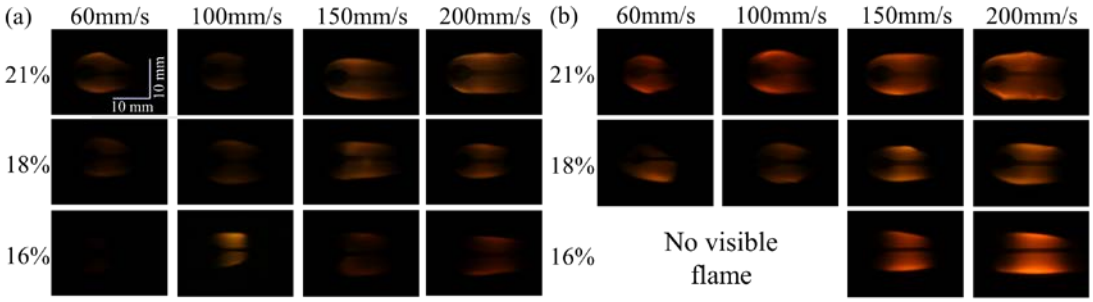

Fig. 3. Frames showing the evolution of the visible flame shape for increasing concurrent flow velocity (from the left to the right) and increasing O_2 concentration (from the bottom to the top): (a) NiCr core wire; (b) Cu core wire.

The flame was situated around the molten insulation and extended along the unburned sample. It was observed that the flame length increased as the external flow velocity increased. For high oxygen concentrations, the flame was luminous and observable for the duration of the experiment. However, for an oxygen concentration of 16%, the flame base became faint blue and difficult to observe, but the molten insulation was moving, thus confirming that the flame was sustained.

3.2. Flame development

Figure 4a shows a series of flame pictures at different times for typical experimental conditions, and Fig. 4b shows the displacement of flame tip, base, and length as a function of time. The flame length is defined as the length of the luminous flame, i.e. the distance between the flame tip and base. G_z means the acceleration of the vertical direction of the airplane. It is given in terms of g_0, which is set to be 9.81 m/s^2.

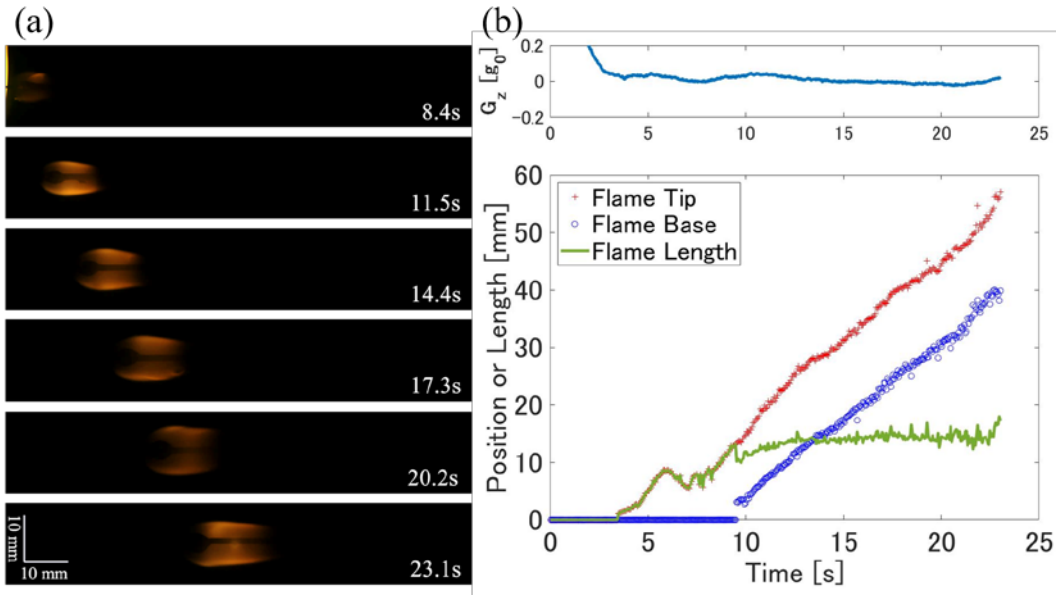

Fig. 4. (a) Frames showing the evolution of the visible flame shape with time after the start of the microgravity period (NiCr core wire; concurrent flow velocity: 150 mm/s; O_2 concentration: 18%). (b) Time variation of gravity level; $g_0 = 9.81$ m/s² (top) and Positions and flame length as a function of time (bottom).

For these experimental settings, the flame front and the flame base spread with almost the same rate, and the resulting flame length is thus constant. This suggests that the concurrent flame spread over wire insulation in microgravity could reach a steady state. Figure 5a shows the backlight images of the flames shown in Fig. 4a, while Fig. 5b shows tracking results for the upstream edge of the molten insulation.

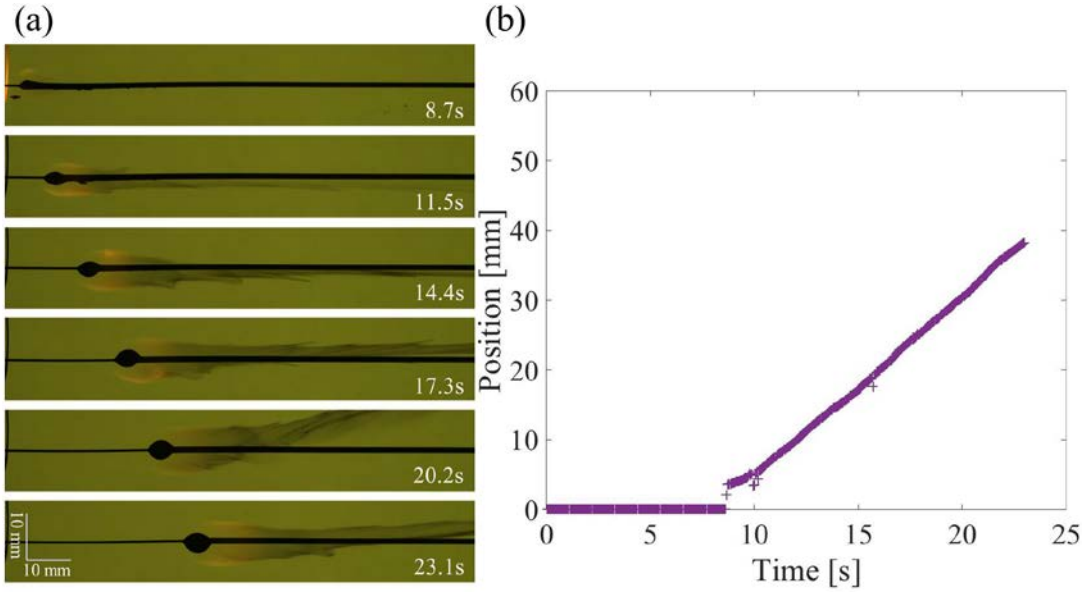

Fig. 5. (a) Frames showing the evolution (time in seconds after the start of the microgravity period) of the coating envelope with backlighting on (NiCr core wire; concurrent flow velocity: 150 mm/s; O_2 concentration: 18%); (b) Position of the upstream molten coating edge versus time, Experimental flame spread rate: 2.6 mm/s.

It can be seen that the displacement of the molten insulation increased linearly, which means that steady movement of the molten insulation was achieved. According to these experimental facts, it is evident that concurrent flame spread over wire insulation in microgravity can be steady.

3.3. Mechanism to attain a steady flame spread

According to Honda et al. [24], flames in concurrent flow achieve a steady spread rate because of transverse heat loss or radiation loss. In the wire case, the transverse heat loss does not exist because the flame is cylindrical.

The following discussion on the mechanism on the presence of steady flame spread is made based on the balance between the energy supply from the flame to the unburned region and the radiation heat

loss from the surface to the ambient. The preheat length is defined as the flame length, and the distance between flame and wire insulation is defined as the flame height. To calculate the flame height (equal to the flame radius r_f) and flame length (L_f), the following equations are introduced, which are based on the model given by Bhattachargee et al. [27], where it is assumed that there is a stoichiometric ratio of fuel and oxidizer.

$$r_f = \left(\frac{\nu V_f \pi (r_s^2 - r_c^2) \rho_s}{\pi V_g \rho_g Y_{O2,\infty}} + r_s^2 \right)^{1/2} \qquad (1)$$

$$L_f = \alpha \frac{V_g (r_f^2 - r_s^2) \ln(r_f / r_s)}{2 D_{o2}} \qquad (2)$$

Here ν, ρ and V are stoichiometric ratio, density and velocity, respectively; r_s and r_c are radius of the inner core and the wire; $Y_{O2,\infty}$ and D_{O2} are respectively the mass fraction of oxygen and diffusion coefficient of oxygen; the subscripts f, g and s denote flame, gas and insulation; α is ratio of the actual flame length and the calculated flame length.

The heat transfer in the preheat zone is defined by the following equation;

$$\dot{Q}_{in} = \dot{Q}_{gs} - \dot{Q}_{rad} = \frac{2\pi\lambda_g (T_f - T_p)}{\ln(r_f / r_s)} L_f - 2\pi r_s \epsilon_s \sigma (T_p^4 - T_\infty^4) L_f \qquad (3)$$

where $\dot{Q}_{gs}$ and $\dot{Q}_{rad}$ are heat conduction rate from flame to insulation and radiation loss rate from insulation surface, respectively; λ_g, ε_s and σ are thermal conductivity of gas phase,

Emissivity, and the Stefan-Boltzmann constant, respectively; T_f, T_p and T_∞ are respectively the flame temperature (assumed to be 1500K for 18% of Oxygen), the pyrolysis temperature, and the ambient temperature.

Also, the required energy to maintain the flame propagation is given as;

$$\dot{Q}_{req} = V_f \pi \{r_c^2 \rho_c c_c + (r_s^2 - r_c^2)\rho_s c_s\}(T_p - T_\infty) \quad (4)$$

where ρ and c are density and specific heat, respectively, while c denotes the core.

Figure 6 shows the change in energy supply from the flame to the sample surface, $\dot{Q}_{in}$ (according to Eq. (3)), as a function of flame spread rate. In addition, the required energy to sustain steady flame spread ($\dot{Q}_{req}$) for different flame spread rates is shown.

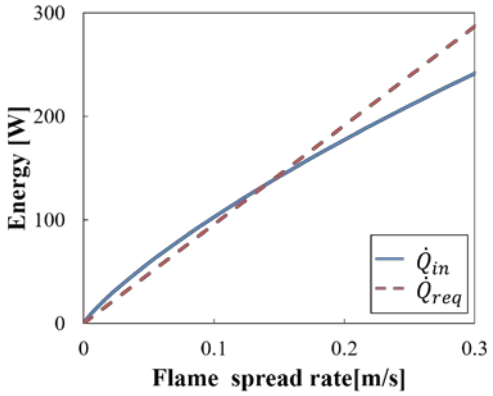

Fig. 6. Variation of energy versus flame spread rate for α=1.0

(Flow velocity: 150mm/s, Oxygen concentration: 18%).

It can be seen in Fig. 6 that the heat supply to the sample, $\dot{Q}_{in}$, is larger than $\dot{Q}_{req}$ for small flame spread rates. This implies that the flame is accelerated to increase its own spread rate because the heat input to the preheat region is larger than $\dot{Q}_{req}$, and the excess heat ($\dot{Q}_{in} - \dot{Q}_{req}$) is used to preheat more fuel than the steadily consumed fuel. However, as the flame spread rate increases, $\dot{Q}_{req}$ becomes larger in proportion to the spread rate, while $\dot{Q}_{in}$ decreases. Eventually, there is an intersection between $\dot{Q}_{in}$ and $\dot{Q}_{req}$. Once the spread rate reaches the intersection, the flame is thermally stable and a steady spread rate is achieved. It means that the presence of a steady condition for the flame spread over the wire insulation was proved based on basic physical understanding (without any

empirical factors).

The backlight picture in Fig. 4 shows that a lot of soot is generated in the flame and released from the downstream of the flame. As a result of such incomplete combustion, the actual flame length should be shorter than that given by the Eq. (2), which assumes complete combustion. The compensation factor of the flame length, α, which denotes the ratio of the actual flame length to the value calculated by Eq. (2) (Fig. 6 shows the case of α=1). Figure 7 shows the value of $\dot{Q}_{in}$ and $\dot{Q}_{req}$ under the otherwise same assumptions, but for α=0.5.

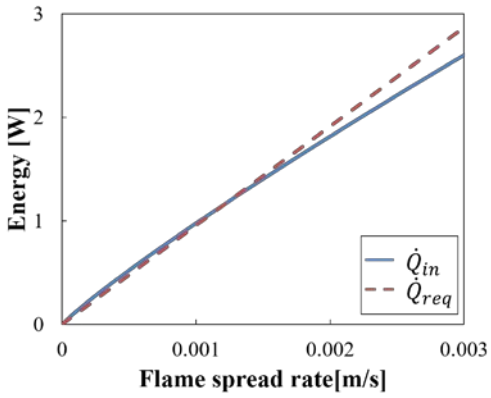

Fig. 7. Variation of energy versus flame spread rate for α=0.5

(Flow velocity: 150mm/s, Oxygen concentration: 18%, Experimental flame spread rate: 2.6 mm/s).

In this case, the calculated flame spread rate needed for the balance point (intersection) is around 1.2 mm/s and the flame length corresponding to the flame spread rate is 11.4 mm. Those values are consistent with the experimental results, while the steady spread rate estimated under the assumption of α=1 (around 150mm/s) is very far from the actual value. These results shows the importance of the correct estimation of the flame length, as inclusion of incomplete combustion estimates resulted in a better agreement between the calculated and the experimental flame spread

rate.

3.4. Steady flame spread rate based on the motion of molten insulation

Figures 8 and 9 show the flame spread rate of NiCr wire and Cu wires. Here, the displacement speed of the upstream edge of molten insulation was used to determine the flame spread rate, because flames in low oxygen concentration are quite dim, and it is thus difficult to distinguish the flame front. Each plot is made up by single experimental results due to the limited number of available microgravity experiments.

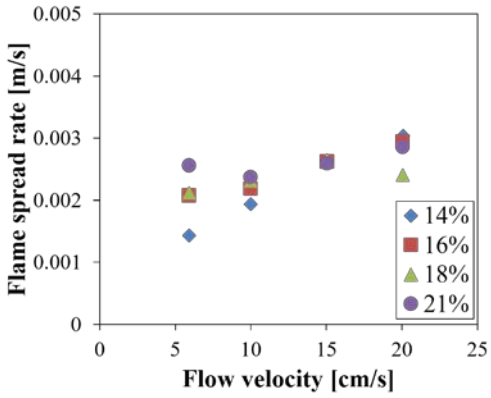

Fig. 8. Steady spread rate (based on the motion of the molten insulation) versus flow velocity for experiments with NiCr wire.

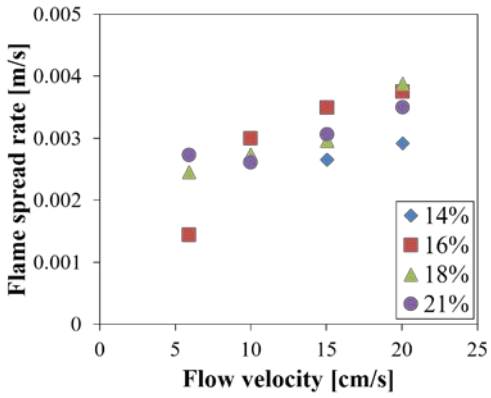

Fig. 9. Steady spread rate (based on the motion of the molten insulation) versus flow velocity for experiments with Cu wire.

For both wire types, the flame spread rate increased as the air flow velocity increased. However, the changes in oxygen concentration had a limited effect on the flame spread rate. When the air flow velocity increases, the flame height decreases and the temperature gradient between the flame and the sample surface increases. As a result, $\dot{Q}_{in}$ (given by Eq. (3)) increases and the radiation heat loss from the sample surface becomes relatively small, which results in increased flame spread rate. Also, the flame spread rate of Cu wire was found to be larger than that of NiCr wire. According to Hu [28], the flame spread rate varies for different core wire materials. This is because the conduction heat supply through the core plays a major role in supporting flame spread. It means that more heat is circulated through the core wire and heat supply from the flame, $\dot{Q}_{in}$, increases rather than the NiCr core wire. Thus, the increased thermal conductivities of the Cu core leads to an increase in the flame spread rate.

3.5. Comparison with normal gravity experiments (upward flame spread)

Experiments in normal gravity were conducted to compare these results with those obtained in microgravity. Figure 10a shows sequential flame images of upward flame spread in normal gravity for a typical experiment, and Fig. 10b shows tracking results of the flame tip, base and length. In these pictures, the direction of gravity is down and the external flow comes from the bottom.

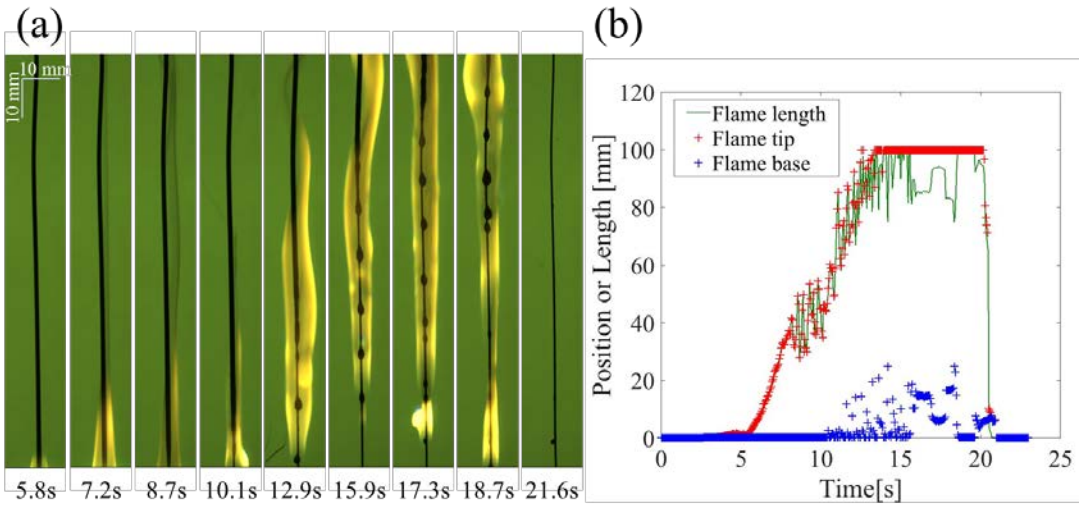

Fig. 10. (a) Frames showing the flame development in 1g (ascending vertical axis is directed upwards) on a NiCr wire for a concurrent flow velocity of 60 mm/s and a O_2 concentration of 21%; (b) Flame base, tip, and length tracking.

As shown in Fig. 10, the positions of the flame tip increased linearly until around 8s. In these experiments, the igniter was turned on until 8s, and the flame shape was observed to be laminar initially. However, after the ignition period, the flame became turbulent and in the flame length increased in an acceleratory manner, until the flame tip eventually reached the edge of the insulation. This means that upward flame spread over the wire insulation in normal gravity cannot reach the steady condition using this sample length even though the flame spreading in concurrent flow in microgravity could reach it. Similar phenomena were observed at 19% oxygen concentration in our experiments. According to Honda [24] and Fernandez-Pello [29], steady state can be achieved in turbulent flow, and there is a possibility for steady flame spread for an infinitely long wire. Further details and discussions on upward flame spread can be found in Fernandez-Pello [29]. However, the flame base did not move downstream, because the molten insulation keeps dripping

while burning. Thus, the flame length became longer with time until the flame tip reached the top edge of the insulation. After that, flame was sustained until the insulation was completely consumed. For every condition, the flame reached the edge of insulation in 15s. For experiments with the sample length shown here, it was not possible to achieve steady flame spread in normal gravity. The major factor for not reaching steady spread is that the condition to obtain heat balance must exist at for very large spread rates, and such a condition requires a long time to be reached. In other words, in normal gravity, the unsteady period on the way to reach steady condition lasts until the flame tip reaches the top end of the sample.

4. Conclusions

The flame spread behavior over wire insulation for concurrent flow in microgravity was studied experimentally. The major conclusions are;

(1) The experimental observation showed that the flame spreading over wire insulation in microgravity could reach a steady state even for external, concurrent flow.

(2) Steady spreading over insulated wire under concurrent flow was explained using the concept of heat balance between heat supply from the flame to the unburned region and required heat to preheat the unburned fuel up to the gasification temperature of the plastic insulation. The analysis showed that there exists a balance point for both heats, which provides the insight of the presence of steady propagation over wire insulation.

(3) The estimated steady spread rate (1.2 mm/s) was consistent with the experimental result by

considering the ratio of the actual flame length to the theoretical to be 0.5. It means that the importance of the correct estimation of the flame length, as inclusion of incomplete combustion estimates resulted in a better agreement between the calculated and the experimental flame spread rate.

(4) The flame spread rate over wire insulation increased around 1-1.5 mm/s as the external concurrent flow velocity increased from 6 cm/s to 20 cm/s. Also, the spread rate for Cu wires was found to be larger than for NiCr wires (around 0.5 mm/s larger for V_g = 10 cm/s and oxygen concentration of 18 %).

(5) In the 1g upward flame spread case, steady flame propagation was not found for the current experimental condition. The flame tip position increased in an acceleratory manner, while the flame base remained at the bottom of the sample and the flame length increased until the flame tip reached the top end of the sample.

Using the above findings, the extinction limit for concurrent flame spread over wire insulation can be predicted, a result that can be used to improve spacecraft fire safety.

Acknowledgments

This research is supported by Japan Space Exploration Agency (JAXA) under the project of FLARE and the Centre National d'Etudes Spatiales (CNES) under contract #130615. The support from the topical team on fire safety in space (ESA-ESTEC contract number 4000103397) is also appreciated. The authors appreciate the contributions of Renaud Jalain and Ulises Rojas Alva during the

parabolic flight experiments.

References

[1] J. Crusan, NASA, available on May 17, 2018 at

https://www.nasa.gov/press-release/nasa-pursues-burning-desire-to-study-fire-safety-in-space

[2] O. Fujita, M. Kikuchi, K. Ito, K. Nishizawa, Proc. Combust. Inst. 28 (2000) 2905–2911.

[3] O. Fujita, K. Nishizawa, K. Ito, Proc. Combust. Inst. 29 (2002) 2545–2552.

[4] S. Takahashi, H. Ito, Y. Nakamura, O. Fujita, Combust. Flame 160 (2013) 1900–1902.

[5] J.M. Citerne, H. Dutilleul, K. Kizawa, M. Nagachi, O. Fujita, M. Kikuchi, G. Jomaas, S. Rouvreau, J.L. Torero, G. Legros, Acta Astronaut. 126 (2016) 500–509.

[6] K. Mizutani, K. Miyamoto, N. Hashimoto, Y. Konno, O. Fujita, Int. J. Microgravity Sci. Appl 35 (2018) 350104.

[7] M. Kikuchi, O. Fujita, K. Ito, A. Sato, T. Sakuraya, Symp. Combust. 27 (1998) 2507–2514.

[8] O. Fujita, T. Kyono, Y. Kido, H. Ito, Y. Nakamura, Proc. Combust. Inst. 33 (2011) 2617–2623.

[9] Y. Takano, O. Fujita, N. Shigeta, Y. Nakamura, H. Ito, Proc. Combust. Inst. 34 (2013) 2665–2673.

[10] M.K. Kim, S.H. Chung, O. Fujita, Proc. Combust. Inst. 33 (2011) 1145–1151.

[11] S.J. Lim, M. Kim, J. Park, O. Fujita, S. Chung, Combust. Flame 162 (2015) 1167–1175.

[12] S. Takahashi, H. Takeuchi, H. Ito, Y. Nakamura, O. Fujita, Proc. Combust. Inst. 34 (2013) 2657–2664.

[13] Y. Nakamura, N. Yoshimura, H. Ito, K. Azumaya, O. Fujita, Proc. Combust. Inst. 32 II (2009)

2559–2566.

[14] A.F. Osorio, K. Mizutani, C. Fernandez-Pello, O. Fujita, Proc. Combust. Inst. 35 (2015) 2683–2689.

[15] O. Fujita, Proc. Combust. Inst. 35 (2015) 2487–2502.

[16] M. Nagachi, F. Mitsui, J. Citerne, H. Dutilleul, A. Guibaud, G. Jomaas, G. Legros, N. Hashimoto, O. Fujita, 47th Int. Conf. Environ. Syst. (2017) 244.

[17] F.A. Williams, Symp. Combust. 16 (1977) 1281–1294.

[18] A.C. Fernandez-Pello, Combust. Sci. Technol. 39 (1984) 119–134.

[19] M.A. Delichatsios, M. Delichatsios, Y. Chen, Y. Hasemi, Combust. Flame 102 (1995) 357–370.

[20] G.H. Markstein, J. de Ris, Symp. Combust. 14 (1973) 1085–1097.

[21] H.T. Loh, C.A. Fernandez-pello, Fire Saf. Sci. 1 (1986) 65–74.

[22] G. Grayson, K.R. Sacksteder, P.V. Ferkul, J.S. T'ien, Microgravity Sci. Technol. VII (1994) 187–195.

[23] X. Zhao, Y.T.T. Liao, M.C. Johnston, J.S. T'ien, P. V. Ferkul, S.L. Olson, Proc. Combust. Inst. 36 (2017) 2971–2978.

[24] L.K. Honda, P.D. Ronney, Proc. Combust. Inst. 28 (2000) 2793–2801.

[25] C.B. Jiang, J.S. Tien, H.Y. Shih, Symp. Combust. 26 (1996) 1353–1360.

[26] A. Guibaud, J.M. Citerne, J.M. Orlac'h, O. Fujita, J.-L. Consalvi, J.L. Torero, G. Legros, Proc. Combust. Inst. (2018) submitted and accepted for Oral presentation, under review.

[27] S. Bhattacharjee, S. Takahashi, K. Wakai, C.P. Paolini, Proc. Combust. Inst. 33 (2011) 2465–2472.

[28] L. Hu, Y. Zhang, K. Yoshioka, H. Izumo, O. Fujita, Proc. Combust. Inst. 35 (2015) 2607–2614.

[29] Fernandez-Pello, A. C. in: G. Cox (Eds), "The Solid Phase," in Combustion Fundamentals of Fire, Academic Press, London, 1995. p. 31–100.

Figure Captions

Fig. 1. Experimental setup: (a) schematic cut of the combustion chamber; (b) picture of a sample on a sample holder.

Fig. 2. Typical frame showing the shape of the flame spreading in a concurrent flow (velocity: 150 mm/s; O_2 concentration: 18%).

Fig. 3. Frames showing the evolution of the visible flame shape for increasing concurrent flow velocity (from the left to the right) and increasing O_2 concentration (from the bottom to the top): (a) NiCr core wire; (b) Cu core wire.

Fig. 4. (a) Frames showing the evolution of the visible flame shape with time after the start of the microgravity period (NiCr core wire; concurrent flow velocity: 150 mm/s; O2 concentration: 18%). (b) Time variation of gravity level; $g_0 = 9.81$ m/s^2 (top) and Positions and flame length as a function of time (bottom).

Fig. 5. (a) Frames showing the evolution (time in seconds after the start of the microgravity period) of the coating envelope with backlighting on (NiCr core wire; concurrent flow velocity: 150 mm/s; O_2 concentration: 18%); (b) Position of the upstream molten coating edge versus time, Experimental flame spread rate: 2.6 mm/s.

Fig. 6. Variation of energy versus flame spread rate for α=1.0 (Flow velocity: 150mm/s, Oxygen concentration: 18%).

Fig. 7. Variation of energy versus flame spread rate for α=0.5 (Flow velocity: 150mm/s, Oxygen concentration: 18%, Experimental flame spread rate: 2.6 mm/s).

Fig. 8. Steady spread rate (based on the motion of the molten insulation) versus flow velocity for experiments with NiCr wire

Fig. 9. Steady spread rate (based on the motion of the molten insulation) versus flow velocity for experiments with Cu wire.

Fig. 10. (a) Frames showing the flame development in 1g (ascending vertical axis is directed upwards) on a NiCr wire for a concurrent flow velocity of 60 mm/s and a O_2 concentration of 21%; (b) Flame base, tip, and length tracking.